

**MAJOR AND TRACE ELEMENT EVIDENCE FOR A 3.26 GA OXYGEN OASIS.** M. M. Tice<sup>1</sup>, C.-T. A. Lee<sup>2</sup> and D. R. Lowe<sup>3</sup>, <sup>1</sup>Department of Geology & Geophysics, Texas A&M University, 3115 TAMU, College Station, TX 77845, tice@geo.tamu.edu, <sup>2</sup>Department of Earth Science, Rice University, MS-126, 6100 Main Street, Houston, TX 77005, ctlee@rice.edu, <sup>3</sup>Department of Geological & Environmental Sciences, Stanford University, Stanford, CA 94305, drlowe@stanford.edu.

**Introduction:** We present evidence for early diagenetic pore fluids with elevated Mn/Fe ratios in 3.26 Ga hematitic sediments. In one case, subsequent evolution of pore fluid composition resulted in lower Mn/Fe ratios. This trend is reflected in compositional zoning of early diagenetic dolomite grains, and most likely reflects release of Mn<sup>2+</sup> to early pore fluids followed by later release of Fe<sup>2+</sup>. This trajectory of pore fluid composition is commonly found in modern reducing sediments, where reduction of Mn(IV) oxides precedes reduction of Fe(III) oxyhydroxides due to Mn(IV)'s greater reduction potential [1]. The sequence of Mn- and Fe-enrichment preserved in these rocks thus probably reflects the early presence of Mn(IV) oxides in the primary sediments. The shallow water mass must have contained at least 10 nM O<sub>2</sub>, if only episodically.

Evidence for oxygenic photosynthesis prior to the oxygenation of the atmosphere at ~2.4 Ga [2] and possibly during earlier oxidative pulses [3] is sparse and controversial [4-9]. Recent experiments demonstrating that anaerobic photoferrotrophs could have produced oxide-facies banded iron formations [10,11] severely limit the usefulness of ferric deposits as markers of O<sub>2</sub> production. Evidence for redox-active manganese cycling at 3.26 Ga therefore places a new and important constraint on the timing of the origin of oxygenic photosynthesis.

**Samples and Methods:** The 3.26–3.23 Fig Tree Group, Barberton greenstone belt (BGB), South Africa, was deposited as fill in a foreland basin [12,13]. Throughout much of the south-central BGB, the Fig Tree Group is represented by mixed siliciclastic and orthochemical shallow-water sedimentary rocks forming a large fan-delta complex, with major outcrops in the Conglomerate Quarry and Barite Valley [13]. These rocks grade laterally into deep-water hematitic banded iron formation (the Manzimnyama Jaspillite) and banded ferruginous chert [13].

Samples of hematitic and ferruginous cherts were collected from both shallow- and deep-water facies of the Fig Tree Group and cut for analysis by x-ray fluorescence microscopy ( $\mu$ XRF) and laser ablation inductively coupled plasma mass spectrometry (LA-ICPMS). Slabs were mapped by  $\mu$ XRF at 100  $\mu$ m and 10  $\mu$ m resolution to identify mineral phases of iron and manganese and to measure Mn/Fe ratios within in-

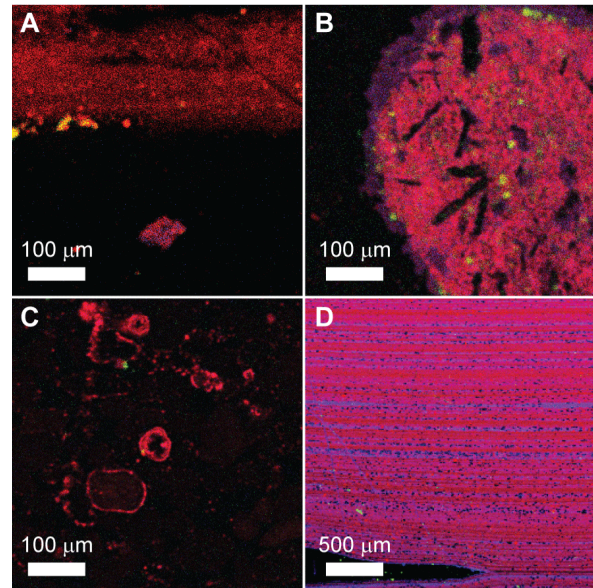


Figure 1. False color images of Fe- and Mn-bearing carbonates from sedimentary rocks of the Fig Tree Group. The red channel intensity is proportional to Fe K $\alpha$ 1 intensity; green channel intensity is proportional to S K $\alpha$ 1 intensity; blue channel intensity is proportional to Mn K $\alpha$ 1 intensity. A) Early diagenetic rhombic dolomite grain (purple) below a hematitic and pyritic layer (red and yellow) from a shallow-water fan-delta sequence in Barite Valley. B) Siderite pebble with dolomite rim (dark purple) from a shallow-water fan-delta sequence in the Conglomerate Quarry. C) Dolomite rims (red) on jasper pellets transported as part of a larger clast to a deep-water setting equivalent to the Manzimnyama Jaspillite. Note concentric layering in thick rims. D) Hematitic (red) and dolomitic laminations (blue-purple) in the Manzimnyama Jaspillite.

dividual grains. Selected samples were analyzed by LA-ICPMS for rare earth element plus yttrium (REY) distributions to characterize precipitating fluids and identify late recrystallization/overprinting events.

**Carbonate Grain Compositions:** Dolomite occurs as isolated rhombic grains, rims on sideritic pebbles and jasper pellets, and fine silty material defining distinct laminations (Fig. 1). REY distributions in all of these materials display some combination of features indicating precipitation, dolomitization, or both, from minimally altered seawater (superchondritic

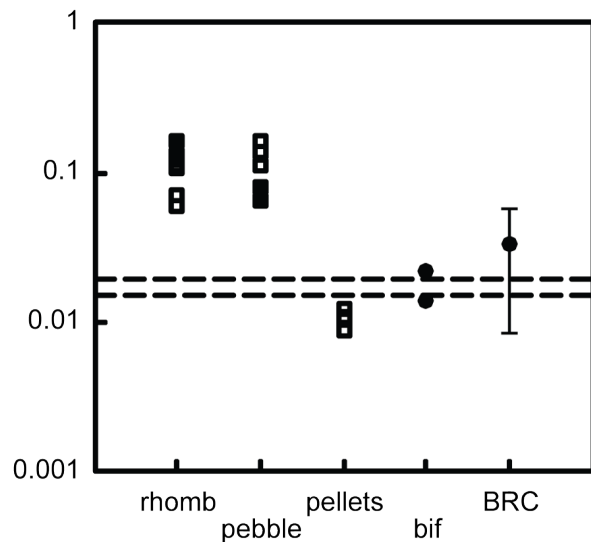


Figure 2. Mn/Fe ratios for Fig Tree Group and Buck Reef Chert (Onverwacht Group) carbonates. Filled circles are from deep-water deposits; filled and open squares are from shallow-water deposits. Open squares indicate measurements on rims defined by distinct mineralogy or Mn/Fe ratio. rhomb = rim and core of rhombic grain from Barite Syncline (Fig. 1A). pebble = dolomite rim and siderite interior of pebble from Conglomerate Quarry (Fig. 1B). pellets = dolomite rims of jasper pellets (Fig. 1C). bif = dolomite laminations in hematitic banded iron formation (Fig. 1D). BRC = bulk rock sideritic samples from the platform and basin facies of the 3.42 Ga Buck Reef Chert (included for comparison). Error bars indicate standard deviation of 13 samples. Dashed lines indicate bulk crust.

Y/Ho ratios, shale-normalized heavy rare earth element enrichment, positive La anomalies [14]), and origins during very shallow burial of the primary sediments. All samples are heavy rare earth element enriched, while Y/Ho ratios vary between chondritic (~28) and seawater-like (~48) [15]. Thus, while all studied carbonates were likely formed during early diagenesis, the Y/Ho ratio provides a potential proxy for relative timing of precipitation within the diagenetic evolution of sediment pore fluids.

Mn/Fe ratios vary from 0.009–0.16 (Fig. 2). In rhombic dolomite grains from shallow-water deposits in Barite Valley, distinct cores and rims are defined by Mn/Fe = 0.13–0.16 and Mn/Fe = 0.06–0.12, respectively (Fig. 1A, Fig. 2). The dolomite rim of the siderite pebble has Mn/Fe = 0.10. In contrast to these ratios which are all above the bulk crustal average of 0.015–0.020 [16,17], dolomite from the banded iron formation has Mn/Fe = 0.014–0.022, and pellet rims have Mn/Fe = 0.009–0.012. Y/Ho ratios are 45 (pellet rims),

44 (banded iron formation), 40 (rhomb core), 35 (rhomb rim), 31 (pebble), and 30 (pebble rim).

**Discussion and Conclusions:** Elevated Mn/Fe ratios in shallow-water early diagenetic dolomite grains could result from either relative Mn<sup>2+</sup> enrichment or relative Fe<sup>2+</sup> depletion. Evolution of pore fluids toward lower Mn/Fe ratios during diagenesis as suggested by zoned rhombic grains in Barite Valley implies that Fe<sup>2+</sup> was not depleted by preferential precipitation of sulfide minerals, which would tend to maintain uniformly low dissolved iron abundances. Similarly, the presence of dolomite rims with seawater-like Y/Ho ratios on jasper pellets suggests that the shallow water mass did not generally have elevated Mn/Fe. It is more likely that elevated Mn/Fe ratios in generations of dolomite having Y/Ho ratios slightly less than modern seawater reflect enrichment of sedimentary pore fluids with Mn<sup>2+</sup>, probably during reduction of primary Mn(IV) oxides. If primary Mn(IV) oxides were produced in the overlying water column at relative rates similar to those of Fe(III) oxide production, then O<sub>2</sub> was the electron acceptor [8]. This suggests that the 3.26 Ga Fig Tree fan delta was episodically exposed to O<sub>2</sub> concentrations sufficient to drive the manganese reducing zone below the sediment surface, or at least 10 nM (8×10<sup>-6</sup> atm) [18].

**References:** [1] Van Cappellen P. and Wang Y. (1996) *Am. J. Sci.*, 296, 197. [2] Bekker A. et al. (2004) *Nature*, 427, 117. [3] Anbar A. D. et al. (2007) *Science*, 317, 1903. [4] Rosing M. T. and Frei R. (2004) *EPSL*, 217, 237. [5] Tice M. M. and Lowe D. R. (2006) *Geol.*, 34, 37. [6] Summons R. E. et al. (1999) *Nature*, 400, 554. [7] Rashby S. E. et al. (2007) *PNAS*, 104, 15099. [8] Rasmussen B. et al. (2008) *Nature*, 455, 1101. [9] Kirschvink J. L. and Kopp R. E. (2008) *Phil. Trans. R. Soc. Lond. B*, 363, 2755. [10] Kappler A. et al. (2005) *Geol.*, 33, 865. [11] Posth N. R. et al. (2008) *Nat. Geosc.*, 1, 703. [12] Jackson M. P. A. et al. (1987) *Tectonophysics*, 136, 197. [13] Lowe D. R. and Nocita B. W. (1999) in Lowe D. R. and Byerly G. R., eds. *GSA Spec. Paper 329*, 233. [14] Kamber B. S. and Webb G. E. (2001) *Geochim. Et Cosmochim. Acta*, 65, 2509. [15] Nozaki Y. et al. (1997) *EPSL*, 148, 329. [16] Weaver B. L. and Tarney J. (1984) in Pollack H. N. and Murthy V. R., eds. *Physics and Chemistry of the Earth*, v. 15, Pergamon, Oxford, 39. [17] Taylor S. R. and McLennan S. M. (1985) *The Continental Crust: Its Origin and Evolution*, Blackwell, Oxford, 312. [18] Canfield D. E. and Thamdrup B. (2009) *Geobiol.*, 7, 385.

**Acknowledgements:** This material is based upon work supported by the National Science Foundation under Award No. EAR-0922108 to MMT.